

TTC22 as a potential prognostic marker and therapeutic target in pancreatic cancer: Insights into immune infiltration and epithelial-mesenchymal transition

YUNTAO DING^{1*}, HUIZHI WANG^{1*}, WENYU CAO^{2*}, TIANYU CAO³,
HAN JIANG¹, ZHENGYUE YU¹, YUJING ZHOU¹ and MIN XU¹

¹Department of Gastroenterology, Affiliated Hospital of Jiangsu University, Jiangsu University, Zhenjiang, Jiangsu 212000; ²Department of Neurology, Affiliated Hospital of Nantong University, Nantong University, Nantong, Jiangsu 226006; ³Department of Urology, Shanghai General Hospital, Shanghai Jiao Tong University School of Medicine, Shanghai 200080, P.R. China

Received August 29, 2023; Accepted October 11, 2023

DOI: 10.3892/ol.2023.14143

Abstract. The mortality rate of pancreatic adenocarcinoma is high, and the effect of traditional treatment is unsatisfactory, thus novel biomarkers are required. Although the important role of tetratricopeptide repeat domain 22 (TTC22) in colon cancer is well established, its precise role in pancreatic cancer remains unclear and requires further investigation. Pan-cancer analysis and single-cell sequencing revealed TTC22 was differentially expressed in various tumors, especially in pancreatic adenocarcinoma. Additionally, clinical data for pancreatic cancer showed a negative association between TTC22 expression and clinical parameters, including survival prognosis. The correlation between TTC22 and immune infiltration in pancreatic cancer was validated by functional enrichment analysis. ESTIMATE and single sample Gene Set Enrichment Analysis algorithms were used to further analyze immune infiltration of TTC22 in pancreatic cancer, and the results suggested that TTC22 inhibited tumor immunity and was negatively correlated with plasmacytoid dendritic cells. Reverse transcription-quantitative PCR further confirmed the differential expression of TTC22 in pancreatic cancer cell lines. Wound healing, Transwell and colony formation assays showed that TTC22 affected the migration and invasion of pancreatic cancer cells. These findings demonstrate that TTC22 may serve as a potential prognostic marker and therapeutic target for the management of pancreatic cancer.

Introduction

Pancreatic carcinoma, a major contributor to cancer-related mortality globally, has witnessed a distressing two-fold increase in its burden over the past 25 years (1). Despite the advent of innovative modalities such as laparoscopic technology and neoadjuvant chemoradiotherapy, the prognosis for patients remains unsatisfactory (2). Moreover, the persisting dearth of molecular and genetic biomarkers guiding clinical decisions concerning patient management is notable (3), despite the demonstrated efficacy of molecular targets such as TP53, CDKN2A and SMAD4 in investigative pursuits (4). Thus, the identification of novel prospective biological markers is of utmost significance.

Tetratricopeptide repeat domain 22 (TTC22), an integral constituent of the TRP gene family, has predominantly been implicated to be involved in colon cancer, where its ability to upregulate WTAP and SNAI1 expression has been shown to facilitate metastasis (5) or participate in the miR663a-TTC22V1 axis, suppressing colon cancer metastasis (6). However, to the best of our knowledge, the ramifications of TTC22 in other malignancies, notably pancreatic carcinoma, have remained unexplored.

Alterations in the tumor microenvironment (TME) exert a profound influence on tumor progression, metastasis and therapeutic response (7). Differential gene expression engenders variations in immune infiltration within tumors, serving as a pivotal mechanism underlying TME modifications (8). Consequently, the precise identification of targeted molecules and the prospective prediction of TME compositions hold great potential for augmenting the effectiveness of immunotherapeutic interventions (9). Nevertheless, the precise implications of TTC22 on immune infiltration within pancreatic carcinoma and its impact on the development of pancreatic cancer cells remain unknown.

Accordingly, in the present study, a comprehensive investigative approach encompassing bioinformatics, single-cell sequencing and cytological experiments was performed to authenticate the distinctive expression patterns of TTC22,

Correspondence to: Professor Min Xu, Department of Gastroenterology, Affiliated Hospital of Jiangsu University, Jiangsu University, 438 Jiefang Road, Zhenjiang, Jiangsu 212000, P.R. China
E-mail: peterxu1974@163.com

*Contributed equally

Key words: tetratricopeptide repeat domain 22, pancreatic cancer, immune infiltration, plasmacytoid dendritic cells

ascertain its clinical relevance and unravel its potential molecular mechanisms in pancreatic carcinoma development. Specifically, by scrutinizing single cell sequencing data and mining The Cancer Genome Atlas (TCGA) and Genotype-Tissue Expression (GTEx) databases, the expression profile, survival prognosis and putative molecular pathways associated with TTC22 in pancreatic carcinoma were corroborated. Moreover, employing single sample Gene Set Enrichment Analysis (ssGSEA) and the ESTIMATE algorithm, the extent of immune infiltration was validated. Additionally, in-depth cytological experiments were performed to further elucidate the ramifications of TTC22 on the carcinogenic progression of pancreatic adenocarcinoma (PAAD) cells.

Materials and methods

Gene expression analysis. A total of 33 different types of tumor project STAR process RNAseq data from TCGA database in the transcripts per million format (<https://portal.gdc.cancer.gov>, accessed on May 12, 2023) were obtained. The GTEx database contains important information regarding healthy tissues and cells, and the information was downloaded. For statistical analysis, the R program ggplot2 (version 3.3.6, <https://ggplot2.tidyverse.org>) was used, together with R software version 4.2.1 (10), car (version 3.1.0) (11) and stats (version 4.2.1, <https://www.r-project.org/>) (10). The Wilcoxon rank-sum test was used to compare the data from the two groups, and $P < 0.05$ was considered to indicate a statistically significant difference. In Table SI, the full tumor names based on the terms used by TCGA are listed.

TTC22 expression in immune subtypes of PAAD. TISIDB (<http://cis.hku.hk/TISIDB/index.php> accessed on 12 April 2023) is a web portal for the analysis of tumor and immune system interaction, integrating multiple heterogeneous data types. This database was used to evaluate the correlation of TTC22 expression in the following immune subtypes of PAAD: C1 (wound healing); C2 (IFN- γ dominant); C3 (inflammatory); C4 (lymphocyte depleted); C5 (immunologically quiet); C6 (TGF- β dominant).

Single-cell sequencing. Cancer Single-cell Expression Map (<https://ngdc.cncb.ac.cn/cancerscem/> accessed on 01 June 2023) was created with the goal of gathering, analyzing and displaying single-cell RNA-Seq data of human cancers (accessed on June 1, 2023 at <https://ngdc.cncb.ac.cn>). To thoroughly examine the tumor microenvironment of several types of human cancer, multi-level analyses were performed and a robust online analysis platform was installed in the database. In database samples, the t-distributed stochastic neighbor embedding (t-SNE) plot displayed the TTC22 expression profile of individual cells.

Survival prognosis analysis. The association between TTC22 expression and overall survival (OS) and disease-specific survival (DSS) of pancreatic tumors was evaluated using Kaplan-Meier plots. The survival package (version 3.3.1, <https://CRAN.R-project.org/package=survival>) was used to perform fitted survival regression and proportional-hazards hypothesis testing, and the ggplot2 and survminer (version 3.3.1,

<https://CRAN.R-project.org/package=survminer>) packages were used to display the findings. When using the log-rank test, $P < 0.05$ was considered to indicate a statistically significant difference.

Clinical significance of TTC22 in PAAD. For further study of the clinical significance of TTC22 in PAAD, diagnostic receiver operating characteristic (ROC) curves, time-dependent area under the curve (AUC), risk score, calibration, nomogram analysis and forest maps were employed. Time-dependent AUC-related data were examined using the timeROC package (version 0.4) (12) and both findings were shown using ggplot2. The pROC package (version 1.18.0) (13), was used for ROC analysis of the data, and the data without clinical information were deleted. Cox regression analysis and proportional hazards hypothesis testing were performed using the survival package, while calibration analysis and visualization were performed using the rms package (version 6.3-0, <https://CRAN.R-project.org/package=rms>). The nomogram correlation model was also built and visualized using the rms package. The ggplot2 package was used to show the forest map and risk score map.

Pan-cancer microsatellite instability (MSI) and mutant-allele tumor heterogeneity (MATH) analysis of TTC22. The UCSC (<https://xenabrowser.net/>) pan-cancer dataset was downloaded, which was carefully standardized. The expression data of the gene ENSG0000006555 (TTC22) were extracted from each sample and screened based on two sources: Primary Blood Derived Cancer-Peripheral Blood and Primary Tumor. The MSI scores for each tumor were obtained from a previous study (14) and integrated with the gene expression data. Additionally, a $\log_2(x+0.001)$ transformation was applied to each expression value. Finally, cancer types with < 3 samples were excluded, resulting in gene expression data for 37 cancer types. For MATH analysis, the UCSC (<https://xenabrowser.net/>) pan-cancer dataset was downloaded, which was carefully standardized. Additionally, the level 4 Simple Nucleotide Variation dataset for all TCGA samples, which was processed by the MuTect2 software (15), was downloaded from GDC (<https://portal.gdc.cancer.gov/>). Using the inferHeterogeneity function of the R package maftools (version 2.8.05) (16), the MATH score for each tumor was calculated. The tumor mutational burden and gene expression data from the samples were integrated and a $\log_2(x+0.001)$ transformation was further applied to each expression value. Finally, cancer types with < 3 samples in a single cancer type were excluded, resulting in expression data for 37 cancer types.

Co-expression gene analysis of TTC22 and functional enrichment in PAAD. According to the expression of TTC22, the data of the relevant molecules were obtained from TCGA in the pancreatic cancer dataset and split into high and low-expression groups (50% vs. 50%). The difference between the initial counts matrix was examined using the DESeq2 (version 1.36.0) (17) and the ggplot2 was used to plot the volcano plots. The top 5 positively correlated genes and the top 5 negatively correlated genes were identified using a heat map and chord diagram, along with Spearman's correlation coefficient. The circlize (version 0.4.1) (18), package was used to show the chord diagram, and ggplot2 was used to plot the heat

maps. Using the clusterProfiler package (version 4.4.4) (19), Kyoto Encyclopedia of Genes and Genomes (KEGG) and Gene Ontology (GO) were used for enrichment analysis, and the GPlot package (version 1.0.2) (20) was used to obtain the zscore value corresponding to each enriched element. clusterProfiler was used for GSEA. ggplot2 was used to display data from KEGG, GO and GSEA.

Immune checkpoint gene profiling and immunomodulatory gene analysis. For immune checkpoint gene profiling, the harmonized pan-cancer dataset was downloaded from UCSC (<https://xenabrowser.net/>): TCGA TARGET GTEx (PANCAN, n=19,131, G=60,499), ENSG00000006555 (TTC22) and 60 two-class immune checkpoint pathway genes (inhibitory for 24 and stimulatory for 36) were extracted from the literature Immune Landscape of Cancer (21) marker gene expression data in each sample, and the sample source was screened for Primary Solid Tumor, Primary Tumor, Primary Blood-Derived Cancer-Bone Marrow, and Primary Blood-Derived Cancer-Peripheral. $\log_2(x+0.001)$ transformation was applied to each expression value, and then the Pearson's correlation coefficient was calculated between ENSG00000006555 (TTC22) and the marker genes of five immune pathways. For immunomodulatory gene analysis, in step one, the harmonized pan-cancer dataset was downloaded from the UCSC (<https://xenabrowser.net/>) database, which was carefully standardized. Furthermore, ENSG00000006555 (TTC22) and 150 immune pathways (including 41 chemokines, 18 receptors, 21 major histocompatibility complex, 24 immune inhibitors and 46 immune stimulators) expression data of marker genes in each sample were further extracted from step one. Furthermore, the sample sources were screened as follows: Primary Solid Tumor, Primary Tumor, Primary Blood-Derived Cancer-Bone Marrow and Primary Blood-Derived Cancer-Peripheral. $\log_2(x+0.001)$ transformation was applied to each expression value. The Pearson's correlation was then calculated between ENSG00000006555 (TTC22) and the marker genes of five immune pathways.

Immune infiltration analysis. The expression levels of TTC22 in pancreatic cancer stroma and immune scores were calculated using the R package, estimate (version 1.0.13, <https://R-Forge.R-project.org/projects/estimate/>) On the basis of the ssGSEA algorithm provided in the R package-GSVA (version 1.46.0) (22), 24 immune-cell markers (23) were annotated to determine specifics of immune infiltrates. Spearman's correlation analysis was used to assess the correlation between the expression levels of TTC22 and immune cell infiltration. Differences in the degree of immune cell infiltration between the high- and low-expression groups were assessed using a Wilcoxon's rank-sum test. The results were visualized using ggplot2.

Cell lines and cell culture. The Jiangsu University School of Medicine's Institute of Basic Medicine and the Central Laboratory of the Affiliated Hospital of Jiangsu University both provided and maintained the pancreatic cancer cell lines PaTu8988, MIA PACA2 and PANC-1. Cells were maintained in a humidified incubator at 37°C supplied with 5% CO₂. Cells were cultured in DMEM (HyClone; Cytiva) supplemented

with 10% FBS and 100 mg/ml penicillin (both from Beyotime Institute of Biotechnology).

Reverse transcription-quantitative PCR. TRIzol® (Invitrogen; Thermo Fisher Scientific, Inc.) was used to extract total RNA (from pancreatic cancer cell lines including PANC-1, MIA PACa2 and PaTu8988 cells). RevertAid first-strand cDNA Synthesis Kit was used for reverse transcription according to the manufacturer's protocol (Thermo Fisher Scientific, Inc.). iQ SYBR Premix Ex Taq Perfect Real Time (Bio-Rad Laboratories, Inc.) and SYBR MasterMix were used for qPCR. β -actin was used as the housekeeping gene. The sequences of the primers were as follows: TTC22 forward, 5'-ATCCACATCAGAGCCTACCTG-3' and reverse, 5'-CGTCCACGCCCA TATAGTAGT-3'; and β -actin forward, 5'-CACGAACTACC TTCAACTCC-3', and reverse, 5'-CATACTCCTGCTTGC TGATC-3'. The sequences of the primers used for the amplification of epithelial-mesenchymal transition (EMT)-related molecules are listed in Table SII. The thermocycling conditions samples for qPCR were: Initial denaturation at 95°C for 3 min, followed by 40 cycles of 20 sec, 56°C for 20 sec and 72°C for 30 sec. The relative expression of genes was calculated using the comparative Cq method ($\Delta\Delta Cq$) and the fold enrichment was determined as follows: $2^{-[\Delta Cq(\text{sample})-\Delta Cq(\text{calibrator})]}$ (24).

Knockdown of gene expression using siRNAs. In the present study, three siRNA constructs targeting TTC22 were obtained from Shanghai GenePharma, Co., Ltd. The specific sequences of the siRNAs are shown in Table SIII. The PANC-1 and PaTu8988 cell lines were used for siRNA transfection. The cell medium was replaced with DMEM without FBS in a cell ultra-clean table, and 100 μ l DMEM was added to each of the two sterile Eppendorf (EP) tubes. In one EP tube, 5 μ l each of the three siRNAs, and in the other EP tube, 5 μ l Lipofectamine® 2000 reagent, was added, gently shaken to fully mix and left for 5 min. The solutions in the two EP tubes were mixed and allowed to stand for 25 min after thorough mixing. The mixture was slowly dropped into the cell culture medium, and the six-well plate was gently shaken to ensure all the solutions were fully mixed. The original medium was discarded and replaced with supplemented DMEM 6 h after incubation with the transfection mix. After a further 48 h, the efficiency of knockdown in the PANC-1 and PaTu8988 cells was verified by qPCR. Subsequent experiments were performed 72 h post-transfection.

Wound healing assays. A total of 1.25×10^5 transfected PaTu8988 and PANC-1 cells/well were seeded for 24 h and cultured with DMEM (HyClone; Cytiva) only. Subsequently, a wound was created by scratching the monolayer of cells using a 10- μ l plastic tip, nonadherent cells were washed away by PBS. With 0 h as the starting time point, 18 h later, the wound was imaged using a brightfield microscope (x10 magnification) connected to a digital camera. The wound healing rate (%) was calculated as follows: $100 \times [(wound\ width\ at\ 0\ h - width\ at\ 20\ h) / width\ at\ 0\ h]$. All experiments were repeated three times.

Transwell migration and invasion assay. According to the manufacturer's instructions, Transwell assays were performed using a Transwell insert (Corning Inc.; 8- μ m pores). PaTu8988

and PANC-1 cells were collected, resuspended in serum-free media, and then added to the upper chamber of the inserts (1×10^5 cells/well). In the lower chamber, supplemented media (10% FBS) and the cells were cultured for 24 h at 37°C . Subsequently, the upper layer of cells was scraped off, and the cells that had migrated to the lower layer were fixed in $500 \mu\text{l}$ 4% paraformaldehyde for 20 min at 26°C and stained with 0.05% crystal violet for 30 min at 26°C . The mean number of cells per field was calculated across five independent fields of view. For the invasion assay, Transwell inserts were pre-coated with Matrigel (BD Biosciences, Inc.), in serum-free media to assess cell invasion at 37°C for 24 h. The number of cells that had invaded were counted in four fields of view ($\times 10$ magnification; brightfield microscopy). All experiments were repeated at least three times.

Colony formation assay. Cells were resuspended in media, transferred to 6-well plates (500 cells/well) and cultured for 10–14 days until colonies were visible at 37°C . To count the number of colonies, cells were fixed in 4% paraformaldehyde for 15 min and stained with 0.05% crystal violet for 30 min at room temperature. When a single cell proliferates *in vitro* for more than six passages, the population of cells composed of its progeny is considered a clonal colony. Clusters of cells consisting of ≥ 50 cells ranging in size from 0.3–1.0 mm were considered colonies. The number of colonies was counted.

Statistical analysis. All data are presented as the mean \pm standard deviation of at least three independent experiments. Two independent groups were analyzed with unpaired Student's t-test. And a one-way ANOVA and Bonferroni's post hoc test was used for comparisons between multiple groups. Kaplan-Meier survival analysis with a log-rank test was used for survival analysis. $P < 0.05$ was considered to indicate a statistically significant difference.

Results

Differential expression of TTC22 in pan-cancer and pancreatic cancer. The relative expression levels of TTC22 in pan-cancer tissues and adjacent normal tissues were assessed, which suggested that TTC22 was differentially expressed in 33 tumors, among which TTC22 was highly expressed in cervical squamous cell carcinoma and endocervical adenocarcinoma (CESC), PAAD, ovarian serous cystadenocarcinoma (OV) and stomach adenocarcinoma (STAD), as well as other tumors (Fig. 1A). Further comparison of TTC22 expression between tumors in single cell public database, Cancer Single-cell Expression Map showed that it was highly expressed in PAAD, OV, STAD and bladder urothelial carcinoma amongst other tumors (Fig. 1B). It was further found that TTC22 expression was significantly higher in pancreatic cancer samples than in normal tissues in TCGA (Fig. 1C). The TISIDB database suggested that TTC22 was highly expressed in different immune subtypes of pancreatic cancer (Fig. 1D). The t-SNE plots also showed the TTC22 pancreatic cancer expression profile was high at the single-cell level and three representative single-cell sequencing results from the single cell public database, Cancer Single-cell Expression Map, were selected (Fig. 1E–G).

Prognostic and clinical significance of TTC22 in pancreatic cancer. The effect of TTC22 on pancreatic cancer prognosis was assessed using Kaplan-Meier curves, which showed that low TTC22 expression was associated with a better prognosis, while high TTC22 expression was associated with a poor prognosis regarding both OS and DSS (Fig. 2A and B). The risk score plot further demonstrated that high TTC22 expression was associated with a poor prognosis in patients with pancreatic cancer (Fig. 2C). In addition, the ROC curve showed that TTC22 expression had good predictive ability in distinguishing patients with pancreatic cancer, with an area under the curve AUC value of 0.893 (95% CI, 0.857–0.929; Fig. 2D). Furthermore, the time-dependent AUC curve suggested that TTC22 expression had good predictive ability for prognostic efficacy from 1–5 years, among which, the best prognostic efficacy was predicted at 3 and 4 years (Fig. 2E). Calibration analysis was used to predict the relationship between TTC22 expression and the 1, 2 and 3-year prognosis in patients with pancreatic cancer to better determine the clinical significance of TTC22 in pancreatic cancer. The survival rate was consistent with the predicted results of the model, and at the same time, TTC22 was used as one of the independent OS factors to construct a prognostic calibration curve for predicting the prognosis of patients with pancreatic cancer (Fig. 2F and G). Finally, univariate and multivariate Cox regression analyses were used to identify the prognostic factors. Univariate prognostic analysis showed that TTC22 expression was significantly associated with tumor complete response (CR) (HR, 0.428; 95% CI, 0.242–0.755; $P = 0.003$). On multivariate analysis, TTC22 expression was also significantly associated with CR stage (HR, 0.428; 95% CI, 0.242–0.755; $P = 0.003$; Fig. 2H–I).

MATH and MSI analysis of TTC22 pan-cancer. For the MATH analysis, the Pearson correlation coefficient in each type of tumor was calculated, and significant correlations were observed in seven tumors, including significant positive correlations in two types of tumors: Stomach and esophageal carcinoma (STES) ($n = 589$, $R = 0.092$, $P = 0.025$) and uterine corpus endometrial carcinoma (UCEC) ($n = 175$; $R = 0.185$, $P = 0.014$). Lung adenocarcinoma (LUAD) ($n = 508$; $R = -0.112$, $P = 0.011$), kidney renal papillary cell carcinoma (KIRP) ($n = 279$; $R = -0.149$, $P = 0.012$), pan-kidney cohort [kidney chromophobe + kidney renal clear cell carcinoma (KIRC) + kidney renal papillary cell carcinoma (KIRP)] (KIPAN) ($n = 679$; $R = -0.415$, $P < 0.01$), KIRC ($n = 334$, $R = -0.307$, $P < 0.01$) and testicular germ cell tumors ($n = 143$, $R = -0.186$, $P = 0.025$) exhibited significant negative correlations with TTC22 (Fig. 3A). For MSI analysis, the Pearson correlation coefficient in each tumor was calculated, and significant correlations were observed in 13 tumors, including significant positive correlations in 5 tumors: Glioma ($n = 657$, $R = 0.091$, $P = 0.020$), LUAD ($n = 511$, $R = 0.108$, $P = 0.014$), STES ($n = 592$, $R = 0.114$, $P = 0.005$), STAD ($n = 412$, $R = 0.222$, $P < 0.01$) and lung squamous cell carcinoma ($n = 490$, $R = 0.105$, $P = 0.02$). Negative correlations with TTC22 were found in CESC ($n = 302$, $R = -0.132$, $P = 0.021$), KIPAN ($n = 688$, $R = -0.254$, $P < 0.01$), prostate adenocarcinoma ($n = 495$, $R = -0.132$, $P = 0.021$), UCEC ($n = 180$, $R = -0.178$, $P = 0.016$), head and neck squamous cell carcinoma ($n = 500$, $R = -0.17$, $P < 0.01$), skin cutaneous

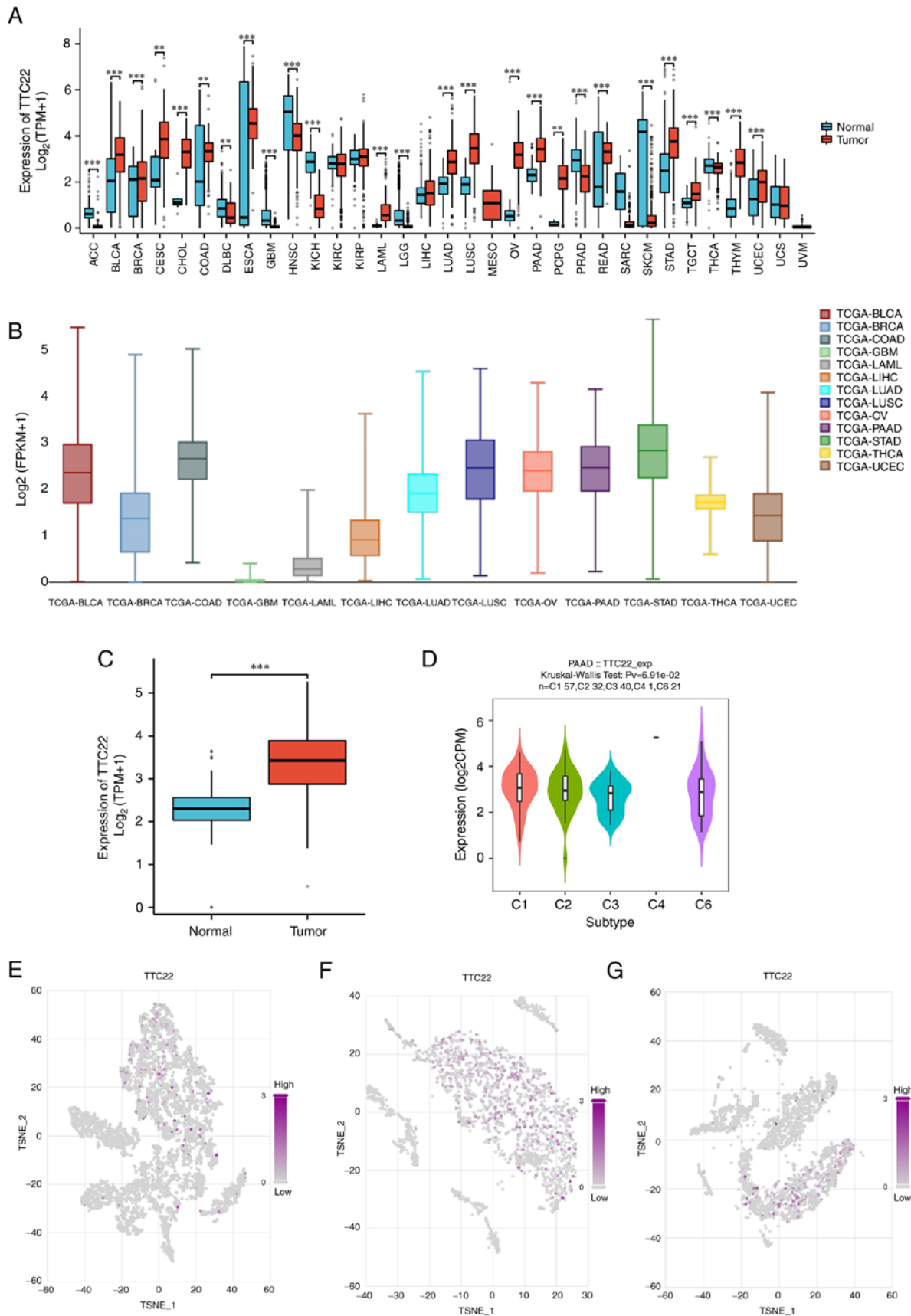


Figure 1. The relative expression of TTC22 pan-cancer and in PAAD. (A) Expression of TTC22 in several types of tumors compared with normal tissues based on data obtained from The Cancer Genome Atlas and Genotype-Tissue Expression. (B) Expression of TTC22 in different types of tumors based on the Cancer Single-cell Expression Map database. (C) Relative expression of TTC22 in pancreatic cancer cells and pancreatic normal cells. (D) Relative expression of TTC22 in different immune subtypes of PAAD. (E-G) Single-cell relative expression of TTC22 in PAAD from three representative single-cell sequencing results for pancreatic cancer were obtained in Cancer Single-cell Expression Map public database. **P<0.01; ***P<0.001. TTC22, tetratricopeptide repeat domain 22; PAAD, pancreatic adenocarcinoma.

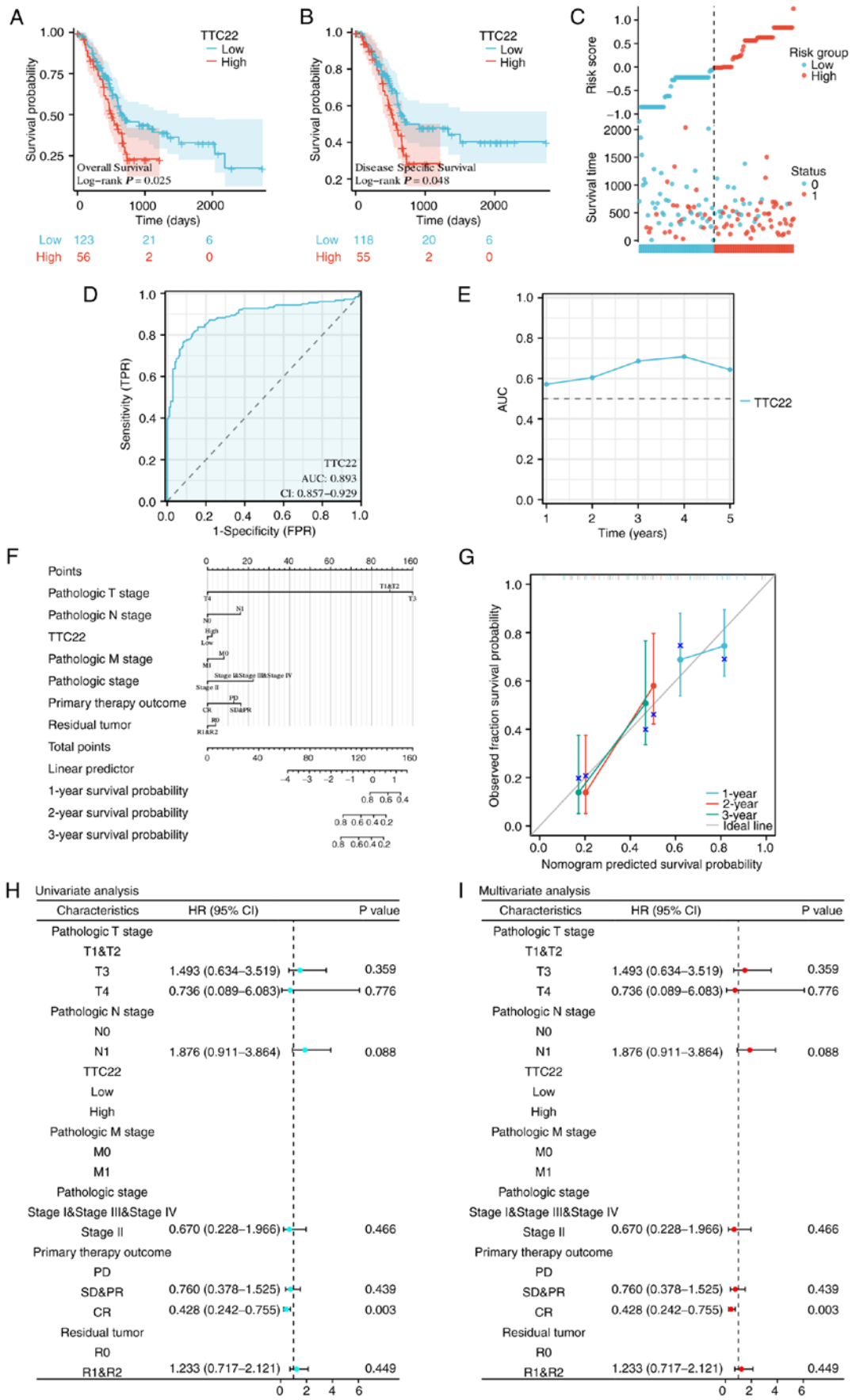


Figure 2. Clinical indicators of TTC22 in pancreatic cancer. (A) Effect of TTC22 expression on the overall survival in PAAD. (B) Effect of TTC22 expression on the disease-specific survival in PAAD. (C) Risk score of TTC22 in PAAD. (D) ROC curve of TTC22 in PAAD. (E) Time-dependent AUC of TTC22 in PAAD. (F) A nomogram for prediction of 1-, 2-, and 3-year overall survival rates of patients with PAAD. (G) Calibration curves of the nomogram prediction of 1-, 2- and 3-year overall survival rates of patients with PAAD. (H) univariate and (I) multivariate analysis in PAAD. TTC22, tetratricopeptide repeat domain 22; PAAD, pancreatic adenocarcinoma; ROC, receiver operating characteristic; AUC, area under the curve.

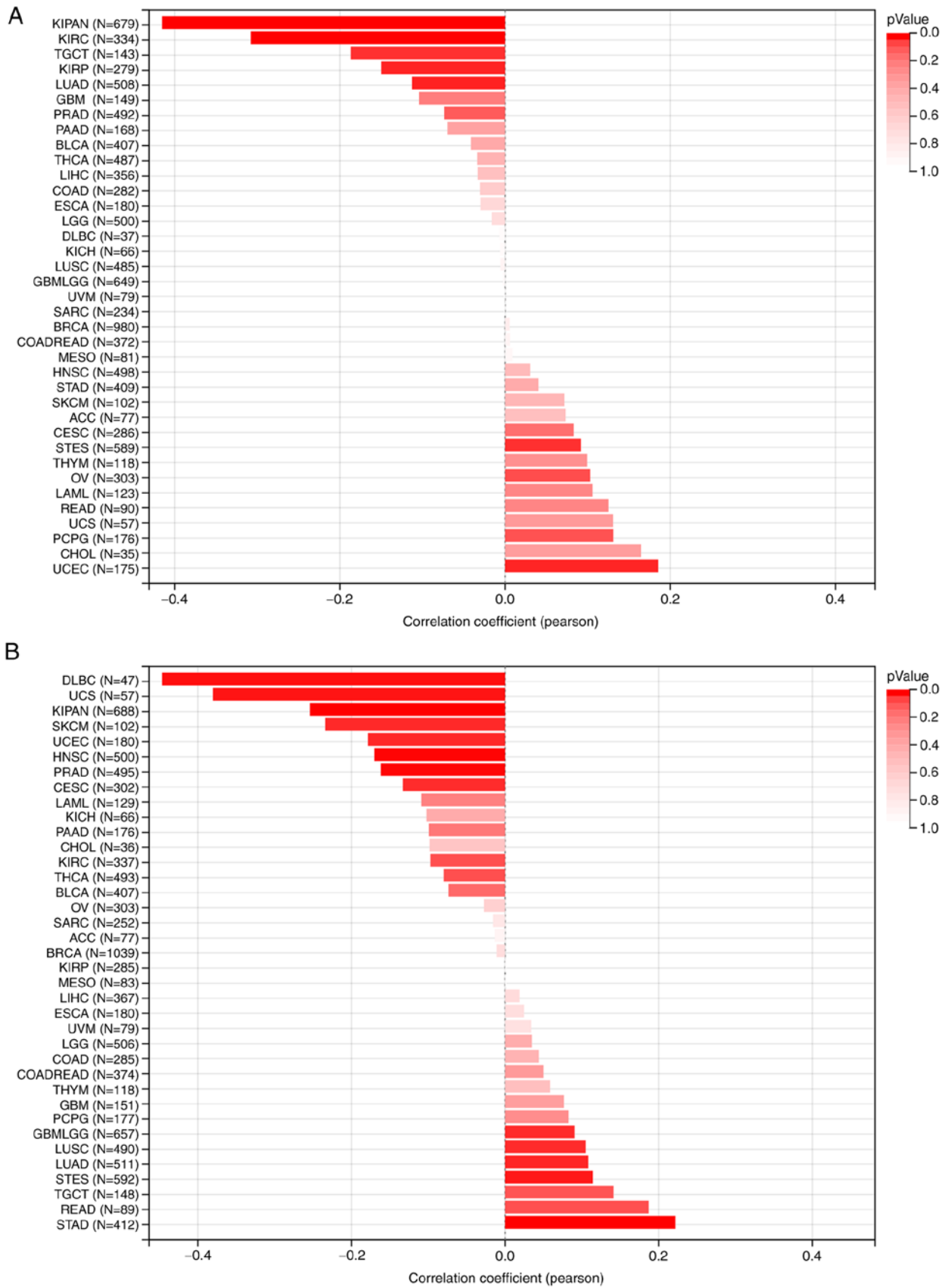


Figure 3. MSI and MATH analysis of TTC22 in pan-cancer. (A) MATH analysis of TTC22 in pan-cancer. (B) MSI analysis of TTC22 in pan-cancer. TTC22, tetratricopeptide repeat domain 22; MSI, microsatellite instability; MATH, mutant-allele tumor heterogeneity.

melanoma (n=102, R=-0.234, P=0.017), uterine carcinoma (n=57, R=0.379, P<0.01) and lymphoid neoplasm

diffuse large B-cell lymphoma (n=47, R=-0.446, P=0.001) (Fig. 3B).

Analysis of differentially expressed genes (DEGs) related to TTC22 and functional enrichment in PAAD. Dseq2 was used to analyze the DEGs associated with TTC22 in PAAD. The results showed that there were 2,118 differentially expressed genes between the TTC22 high-expression group and the TTC22 low-expression group, including 949 upregulated genes and 2,019 downregulated genes [$P < 0.05$; $|\text{Log}_2\text{-FC}| > 1$; Fig. 4A). The relationship between the top 5 highly expressed DEGs and the top 5 low expression DEGs (including downregulated PNLIP, CLPS, CPA1, C6orf58 and AMY2A, and upregulated RETNLB, REG4, AC012317.2, MUC2, KRT4) is shown in Fig. 4B and C. Furthermore, KEGG, GO and GSEA were used to explore the functional enrichment. In the GO enrichment, the terms were primarily enriched in 'humoral immune response', 'digestion', 'immunoglobulin production', 'antigen receptor-mediated signaling pathway', 'T cell receptor complex', 'plasma membrane signaling receptor complex', 'immunoglobulin complex', 'external side of plasma membrane', 'antigen binding', 'receptor ligand activity', 'gated channel activity' and 'signaling receptor activator activity'. For KEGG, the primarily enriched terms were 'neuroactive ligand-receptor interaction', 'pancreatic secretion', 'retinol metabolism', 'hematopoietic cell lineage', and 'fat digestion and absorption'. For GSEA, the primarily enriched terms were 'o-linked glycosylation of mucins', 'drug metabolism other enzymes', 'oxidation by cytochrome p450', 'cytochrome p450 arranged by substrate type', 'phase i functionalization of compounds', 'retinol metabolism', 'metapathway biotransformation phase I and II', 'biological oxidations', 'digestion and absorption', and 'digestion' (Fig. 4D-F). These results showed that TTC22 was associated with immunoinfiltration and EMT in pancreatic cancer.

Correlation between TTC22 expression levels and immune checkpoint genes and immune-related genes pan-cancer. As shown in Figs. 5A and 6A, it was suggested that TTC22 was positively correlated with most immunomodulatory genes in the pan-cancer analysis. Similarly, TTC22 was positively correlated with the majority of the immune checkpoint genes in the pan-cancer analysis. In pancreatic cancer, the trend was not consistent with the majority of tumors; however, ~50% of immune-related genes and immune checkpoint genes were negatively correlated with the expression of TTC22 (Figs. 5A and 6A).

Correlation between TTC22 expression levels and immune infiltration. Spearman's correlation using the ESTIMATE algorithm showed that the expression of TTC22 was negatively correlated with ImmuneScore ($R = -0.365$), StromalScore ($R = -0.424$), and ESTIMATEScore ($R = -0.424$) (Fig. 7A), and this was also observed using box plots (Fig. 7C-E). The relationship between TTC22 expression and 24 types of immune cells in PAAD was assessed, and it was mainly negatively associated with plasmacytoid dendritic cells (pDCs), follicular helper T cells (TFH cells) and T $\gamma\delta$ (Tgd) cells, which were the top three immune cells (Fig. 7B). The correlation coefficients of TTC22 enrichment with three immune cells were as follows: pDCs ($R = -0.510$, $P < 0.001$), TFH cells ($R = -0.432$, $P < 0.001$), and Tgd cells ($R = -0.358$, $P < 0.001$) (Fig. 7I-K); the

enrichment scores exhibited the same trend as the correlation coefficients (Fig. 7F-H). In addition, by analyzing the 10 Hub-genes co-expressed with TTC22, it was found that C6orf58 was negatively correlated with TTC22 (Fig. S1A), while the immune infiltration analysis of C6orf58 suggested that it was positively correlated with pDC immune infiltration (Fig. S1B). The negative correlation between TTC22 and pDC immune infiltration may thus be related to the role of a TTC22-C6orf58 axis.

Relative expression of TTC22 in PAAD cell lines. TTC22 was found to be differentially expressed in pancreatic cancer cell lines by RT-qPCR, with the highest expression levels in PANC-1 cells, the second highest in MIA PACa2 cells and the lowest in PaTu8988 cells (Fig. 8A). Based on the expression levels of TTC22 in the three pancreatic cancer cell lines, PaTu8988 and PANC-1 were selected as cell lines for further experiments. The effectiveness of si-TTC22 (including siTTC22 1, 2 and 3), which was used to knock down TTC22 expression in PaTu8988 and PANC-1 cell lines, is shown in Fig. 8B.

Effect of TTC22 on the migration and invasion of PAAD cells. Cell migration was assessed using a wound-healing assay. TTC22 expression was knocked down in PaTu8988 and PANC-1 cell lines, and the migratory ability of the si-TTC22 cells was significantly lower compared with the si-NC group (Fig. 8C and D). Transwell experiments further showed a decrease in the migratory and invasive ability of the TTC22 knockdown cells. When TTC22 was knocked down in PaTu8988 and PANC-1 cells, it was found that the si-TTC22 cells exhibited reduced invasion and migration compared with the respective control cells (Fig. 9A and B).

Effect of TTC22 on pancreatic cancer proliferation. The effect of TTC22 on the proliferation and colony formation ability of cells was assessed using colony formation assays. TTC22 knockdown in PaTu8988 and PANC-1 cells significantly reduced the proliferation and colony formation of cells compared with the respective control cells (Fig. 9C and D). The differential expression of EMT-related molecules in the control si-NC group of PANC-1 cells compared with the respective TTC22 knockdown cells is shown in Fig. S2. The results showed an oncogenic role for TTC22 in PAAD progression.

Discussion

Pancreatic cancer has emerged as one of the most lethal types of cancer, and is characterized by high mortality rates and an increasing incidence (25,26). Early detection and targeted therapy facilitated by the discovery of effective biological markers have significantly improved patient outcomes (27,28). Notably, molecules such as METTL3 and calcium/calmodulin-dependent protein kinases have been identified as influential factors in the initiation and progression of pancreatic cancer cells, thus representing potential biological markers (29,30). Nevertheless, there remains a need to identify additional markers with diagnostic and therapeutic relevance.

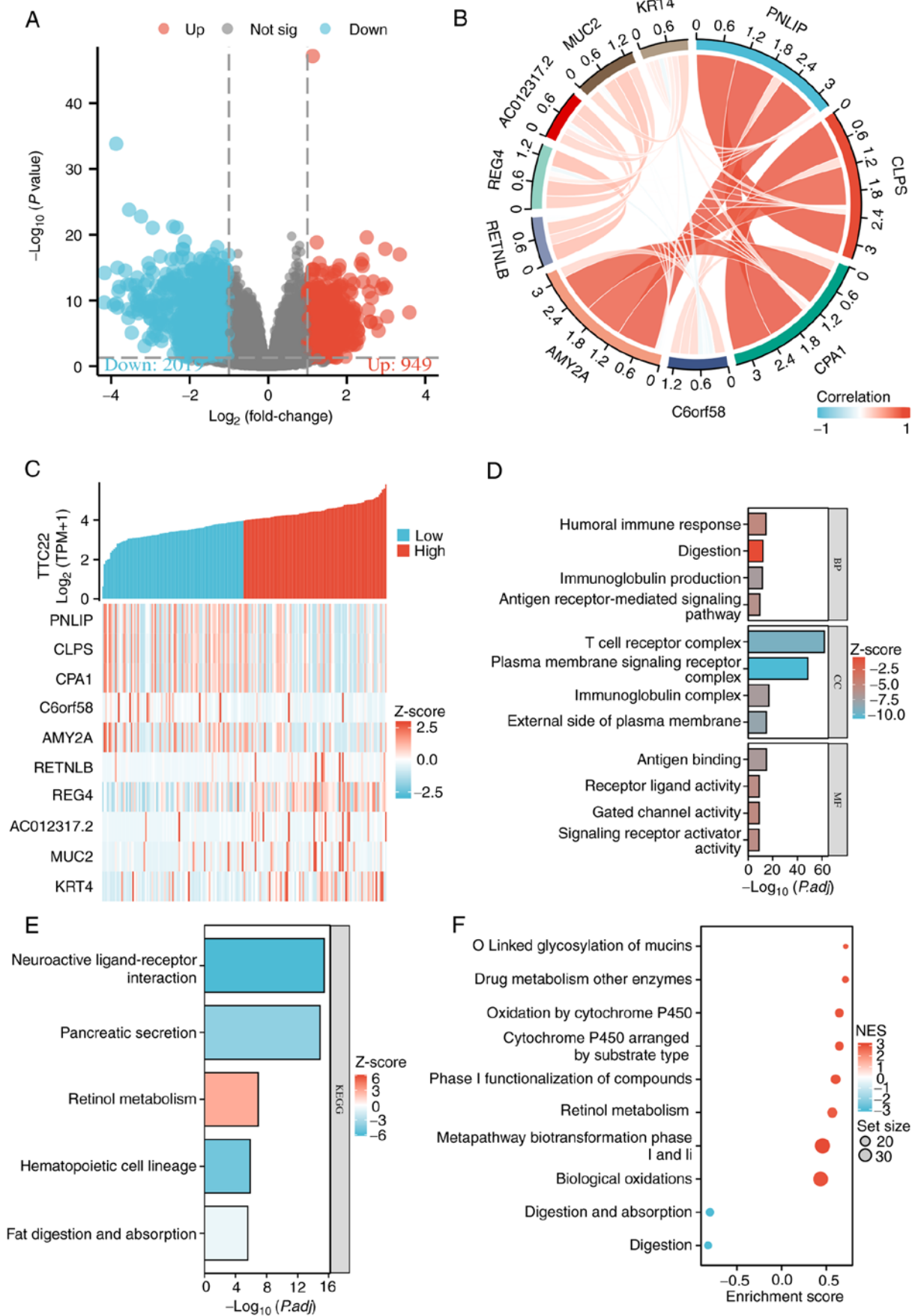


Figure 4. Functional enrichment of DEGs based on TTC22 expression. (A) The volcano plot of the top 10 DEGs based on TTC22 expression using data obtained from The Cancer Genome Atlas ($\log_2\text{FC} > 1$ or < -1). (B) Chord diagram of top 10 DEGs. (C) Correlation heatmap of top 10 DEGs in PAAD. (D) Gene Ontology analysis of TTC22 and the co-expressed genes in PAAD. (E) Kyoto Encyclopedia of Genes and Genomes analysis of TTC22 and the co-expressed genes in PAAD. (F) Gene Ontology analysis and Gene Set Enrichment Analysis of TTC22 and the co-expressed genes in PAAD. TTC22, tetratricopeptide repeat domain 22; DEG, differentially expressed gene; PAAD, pancreatic adenocarcinoma.

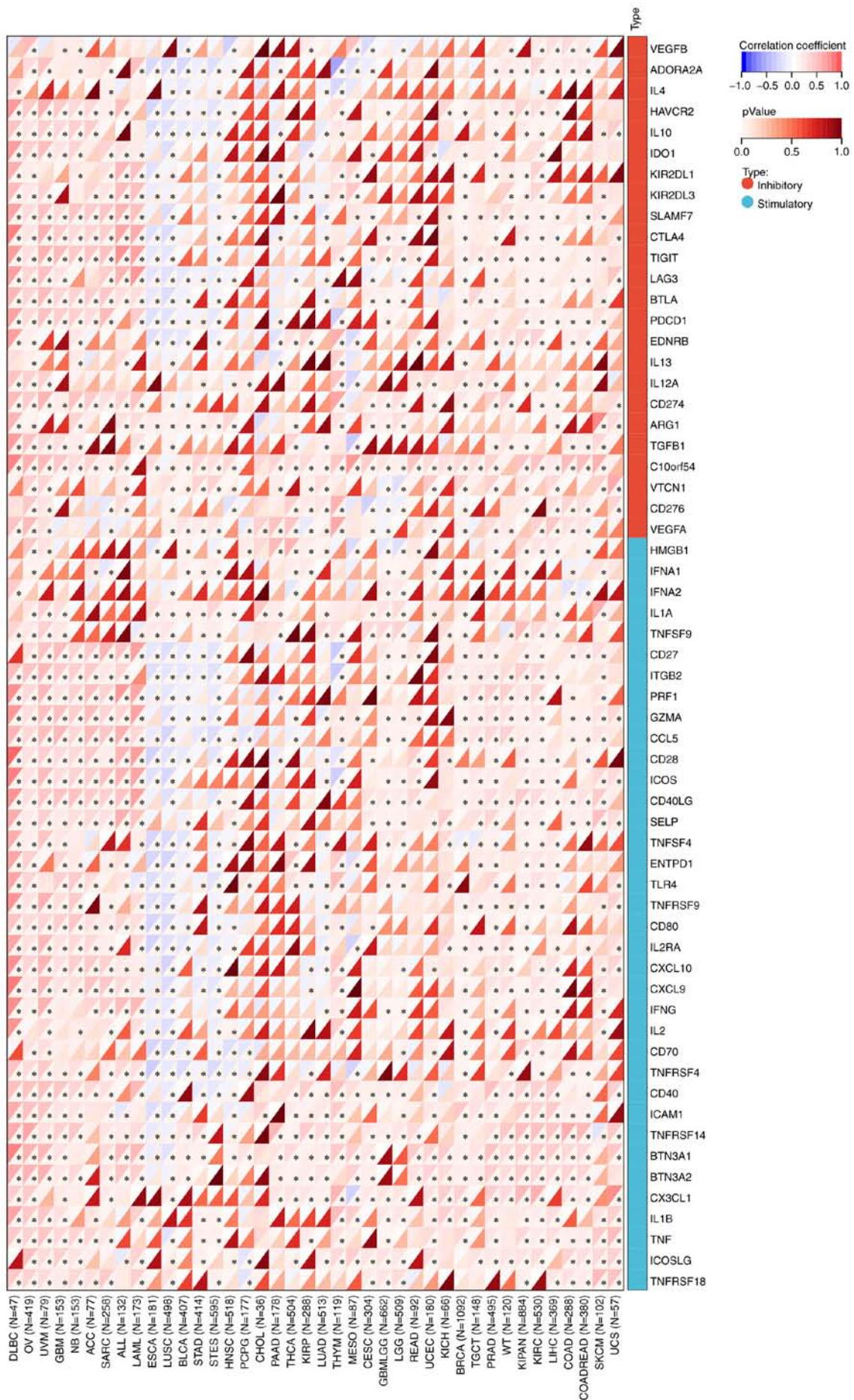


Figure 5. Association of TTC22 with immune checkpoint genes in pan-cancer analysis of TTC22. TTC22, tetratricopeptide repeat domain 22. *P<0.05.

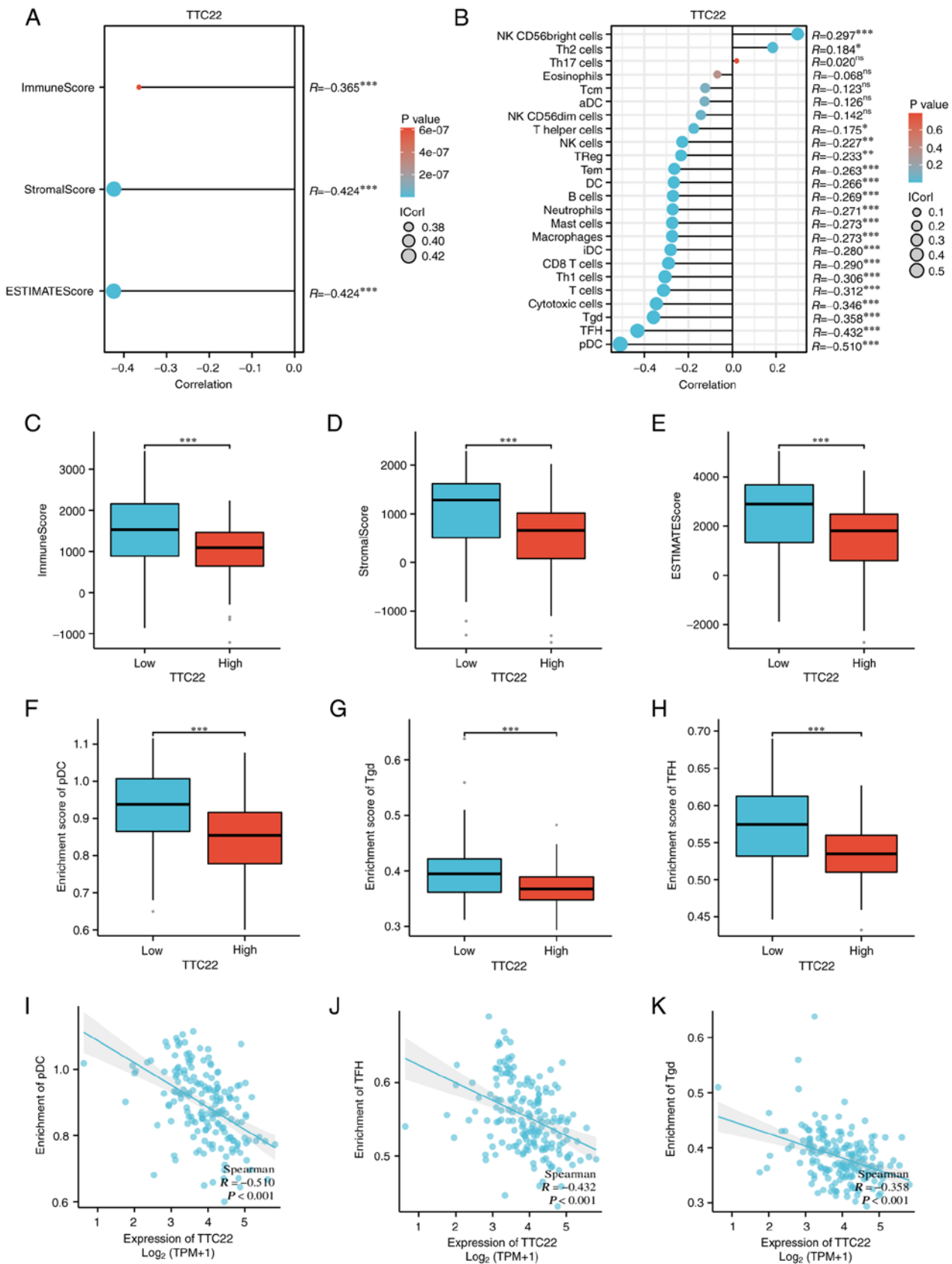


Figure 7. Relationship between TTC22 expression and immune infiltration in pancreatic cancer based on two methods of assessment. (A) Relationship between TTC22 expression and immune infiltration using ESTIMATE. (B) Correlation between TTC22 expression and relative abundance of 24 types of immune cell. The size of the dots corresponds to the absolute Spearman's correlation coefficient values. (C) The relationship between TTC22 expression and ImmuneScore. (D) The relationship between TTC22 expression and StromalScore. (E) The relationship between TTC22 expression and ESTIMATEScore. (F) The relationship between TTC22 expression and enrichment score of pDC. (G) The relationship between TTC22 expression and enrichment score of Tgd. (H) The relationship between TTC22 expression and enrichment score of TFH. (I) The correlation between TTC22 expression and enrichment of pDC. (J) The correlation between TTC22 expression and enrichment of TFH. (K) The correlation between TTC22 expression and enrichment of Tgd. * $P<0.05$; ** $P<0.01$; *** $P<0.001$. TTC22, tetratricopeptide domain 22.

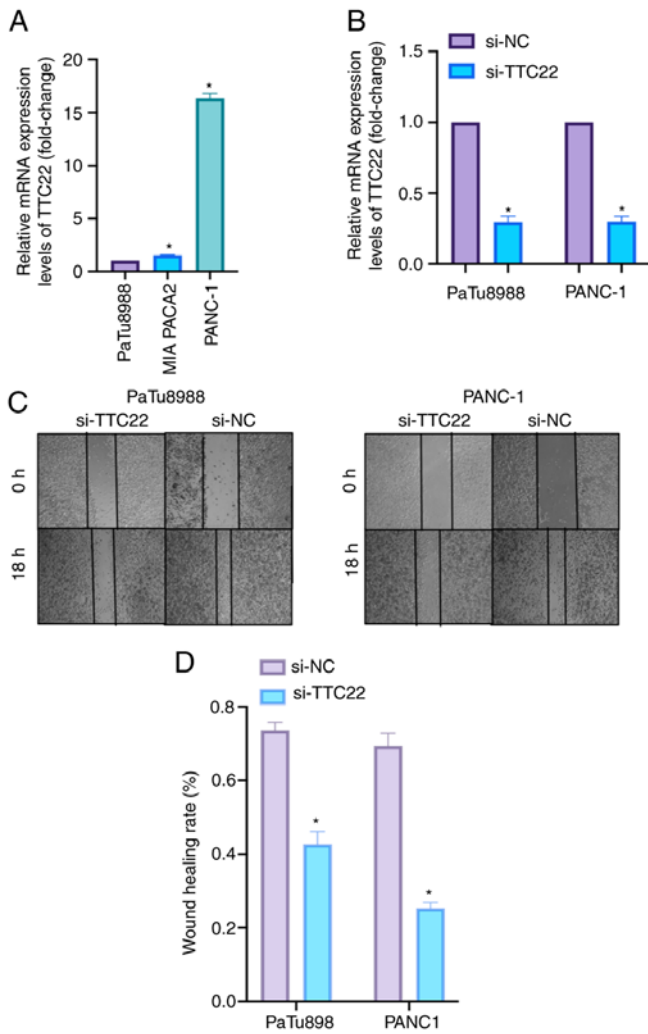


Figure 8. Effect of TTC22 on pancreatic cancer proliferation. (A) Relative expression of TTC22 in pancreatic cancer cell lines. (B) Knockdown of TTC22 in PAAD cell lines. (C) Wound healing assays following TTC22 knockdown in PaTu8988 pancreatic cancer cells (x10 magnification). (D) Wound healing assays following TTC22 knockdown in PANC-1 pancreatic cancer cells (x10 magnification). *P<0.05. TTC22, tetratricopeptide repeat domain 22; PAAD, pancreatic adenocarcinoma; si, small interfering; NC, negative control.

TTC22 belongs to the TRP protein family, which facilitates protein-protein interactions and engages with a range of ligands or substrates, and is thereby implicated in various diseases (31). In the context of tumors, the TRP protein family has been associated with the nuclear export of tRNA, protein synthesis and cell growth (32). For example, TRPV1 has been identified as a potential tumor suppressor and has been found to positively correlate with an anti-tumor immune response in pan-cancer analyses (33), whereas TRV6, in collaboration with NFATC2, promotes breast cancer metastasis (34). However, there is a dearth of research exploring the role of TTC22 in most types of cancer, including pancreatic cancer.

Drawing from the aforementioned research, it was hypothesized that TTC22 may exert influence on the initiation and progression of pancreatic cancer cells, and thus may hold promise as a valuable biological marker and therapeutic target. To gain further insights into the clinical significance of TTC22 in pancreatic cancer, a comprehensive pan-cancer analysis of its expression patterns, with a specific focus on

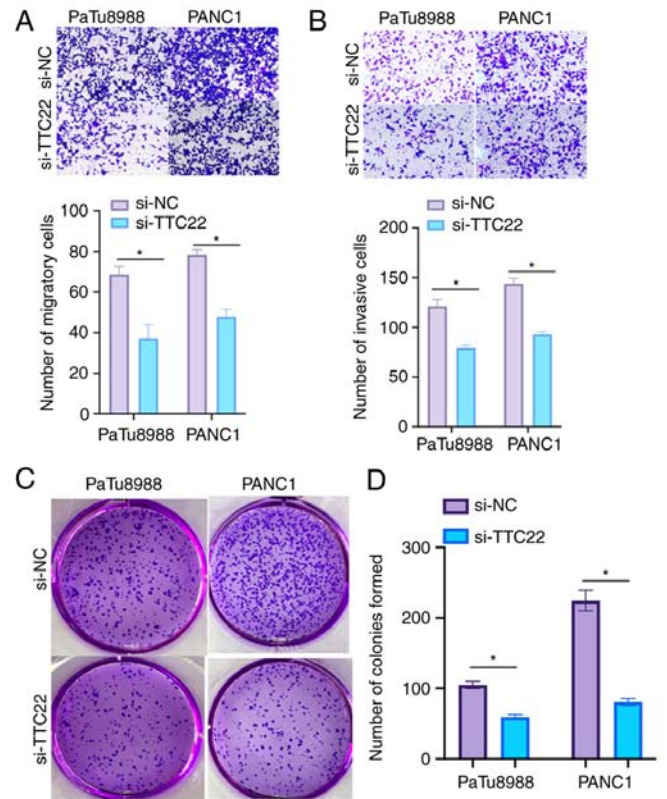


Figure 9. Cytological experiments assessing the effects of TTC22. (A) Migration and (B) invasion of PaTu8988 and PANC-1 cells following TTC22 knockdown. (x10 magnification). (C) Colony formation assays of PaTu8988 and PANC-1 cells following TTC22 knockdown. (x10 magnification). (D) A bar plot of the number of colonies of PaTu8988 and PANC-1 cells following TTC22 knockdown. *P<0.05. TTC22, tetratricopeptide repeat domain 22; si, small interfering; NC, negative control.

pancreatic cancer, utilizing data from TCGA and GTEx was performed. Subsequently, its clinical relevance was assessed by constructing various clinical models, including Kaplan-Meier curves, hazard ratio plots, column line plots, calibration plots, as well as univariate and multivariate Cox regression analyses. Moreover, techniques such as tumor microsatellite instability analysis, assessment of tumor heterogeneity and t-SNE plots based on single-cell sequencing data were used to gain a deeper understanding of the role of TTC22 in tumor biology. The present findings indicated that TTC22 may serve as a novel biological marker for pancreatic cancer. Functional enrichment analysis of genes co-expressed with TTC22 in pancreatic cancer showed that such T-cell receptor complex, antigen binding and immunoglobulin complex may promote pancreatic cancer immune infiltration and serve an important role in tumor biology.

Immunotherapeutic approaches for pancreatic cancer, such as monotherapy immune regulation, have demonstrated limited efficacy in clinical settings and often necessitate combination therapy with other treatment modalities (35,36). Therefore, an analysis of potential immune infiltrates associated with pancreatic cancer biomarkers is imperative. To address this, the relationship between TTC22 and immune checkpoint genes, as well as immune-related genes across various cancer types was analyzed. Additionally, the ssGSEA algorithm was utilized to enrich the profiles of 24 immune cell

types. The results indicated a predominantly negative correlation between TTC22 and immune cells in pancreatic cancer, particularly pDCs.

pDCs belong to the DC family, and serve a pivotal role in initiating cellular and humoral immune responses, and safeguarding the body against infectious diseases and tumor infiltration (37). The robust capacity of pDCs to initiate and regulate adaptive immune responses forms the foundation for generating successful anti-tumor immune responses (38) and has long been a focal point in cancer immunotherapy (39). In liver cancer, inhibition of DC cell increases the likelihood of immune evasion (40), while in pancreatic cancer, restoration of pDC function is associated with disease progression and sensitivity to radiotherapy (41). Hence, it was hypothesized that TTC22 inhibits tumor immune processes in pancreatic cancer and modulates the tumor microenvironment by altering immune cell infiltration, thereby establishing its association with pancreatic cancer as an immune-related biomarker. Furthermore, in pan-cancer analysis of TTC22 and tumor immune cells, it was found that the expression of TTC22 was correlated with the immune infiltration of a variety of tumor cells. It was hypothesized that this may be related to the different target molecules of TTC22 in different types of cancer, and its downstream secreted proteins recruit immune cells to alter the tumor immune microenvironment; this is an important direction that is deserved of further study.

EMT is a cellular program involved in a variety of biological processes and has been shown to play an important role in a variety of tumors (42-44). In the present study, the differential expression of TTC22 in pancreatic cancer cell lines was assessed using RT-qPCR. Moreover, functional assays, including wound healing, Transwell and colony formation assays, were performed to demonstrate the influence of TTC22 on the migration, invasion and development of pancreatic cancer. However, considering that the relative expression levels of TTC22 in PANC-1 cells were still higher than those in PaTu8988 cells after siRNA knockdown of TTC22. Therefore, the genes co-expressed with TTC22 should be further analyzed and screened for validation in clinical samples and animal models, with the aim of identifying genes that are co-downregulated with TTC22 that also affect proliferation and migration. It is plausible that the absolute expression levels of TTC22 mRNA may not be directly correlated with the proliferation and migration of the two cancer cell types. Other genes may also be involved in cell proliferation and migration. This requires further exploration in future studies.

Notably, it is important to acknowledge several limitations of the present study. Firstly, the analysis was primarily based on online databases, namely TCGA and GTEX, with *in vitro* validation limited to pancreatic cancer cell lines, lacking corresponding clinical samples. Secondly, elucidating the specific molecular mechanisms by which TTC22 affects immune infiltration of pDCs in pancreatic cancer warrants further investigation, possibly employing techniques such as western blotting. Moreover, the establishment of appropriate animal models will be crucial to unravel the mechanisms underlying the actions of TTC22 in pancreatic cancer. Thus, in future studies, clinical samples will be used to verify the accuracy of the bioinformatics prediction results, and explore

the potential downstream metabolites by flow cytometric sorting and metabolomics-related sequencing. Additionally, a mouse pancreatic cancer model will be used to verify the downstream pathways and specific mechanisms after knocking down TTC22 expression. In summary, the validity and reliability of bioinformatics in clinical samples and the potential downstream molecules and products will be assessed in future studies. After identifying the target molecules, animal and cell models will be constructed to further confirm these conjectures and verify the underlying molecular mechanisms *in vivo* and *in vitro*.

In conclusion, the present study elucidated the potential role of TTC22 in pancreatic cancer through comprehensive bioinformatics analyses, supported by a series of analytical *in vitro* techniques. TTC22 was revealed to serve a significant role in various aspects of pancreatic cancer, particularly immune infiltration. By influencing the immune infiltration of pDCs, it may hinder tumor immune responses, promote metastasis and contribute to a poor prognosis. Thus, TTC22 holds substantial biological value as a novel therapeutic target in pancreatic cancer.

Acknowledgements

The authors would like to thank Dr Yuqiang Pei (Department of Neurology, Affiliated Hospital of Nantong University, Nantong University, Nantong, China) for their assistance in manuscript writing and figure preparation.

Funding

This study was supported by the National Natural Science Foundation of China (grant nos. 82072754 and 32170910), Jiangsu Provincial Key Research and Development Program (grant no. BE2018689), Natural Science Foundation of Jiangsu Province (grant no. BK20211124), Postgraduate Research & Practice Innovation Program of Jiangsu Province (grant no. KYCX22_3711), and Zhenjiang Key Research and Development Program (grant nos. SH2021037 and SH2018033).

Availability of data and materials

The datasets generated and/or analyzed during the current study are available in TCGA repository, <https://www.cancer.gov/ccg/research/genome-sequencing/tcga>. Other datasets used and/or analyzed during the current study are available from the corresponding author on reasonable request.

Authors' contributions

YD, HW and WC were major contributors in writing the manuscript. YD and HW performed the *in vitro* experiments and designed the study. YD and WC performed the bioinformatics analysis. TC, HJ, ZY, and YZ edited the manuscript, analyzed the data and confirm the authenticity of all the raw data. MX designed the study, interpreted the results, obtained the main financial support, and edited and revised the manuscript. All authors have read and approved the final manuscript.

Ethics approval and consent to participate

Not applicable.

Patient consent for publication

Not applicable.

Competing interests

The authors declare that they have no competing interests.

References

- Klein A: Pancreatic cancer epidemiology: Understanding the role of lifestyle and inherited risk factors. *Nat Rev Gastroenterol Hepatol* 18: 493-502, 2021.
- McGuigan A, Kelly P, Turkington RC, Jones C, Coleman HG and McCain RS: Pancreatic cancer: A review of clinical diagnosis, epidemiology, treatment and outcomes. *World J Gastroenterol* 24: 4846-4861, 2018.
- De Dosso S, Siebenhüner AR, Winder T, Meisel A, Fritsch R, Astaras C, Szturz P and Borner M: Treatment landscape of metastatic pancreatic cancer. *Cancer Treat Rev* 96: 102180, 2021.
- Qian Y, Gong Y, Fan Z, Luo G, Huang Q, Deng S, Cheng H, Jin K, Ni Q, Yu X and Liu C: Molecular alterations and targeted therapy in pancreatic ductal adenocarcinoma. *J Hematol Oncol* 13: 130, 2020.
- You A, Tian W, Yuan H, Gu L, Zhou J and Deng D: TTC22 promotes m6A-mediated WTAP expression and colon cancer metastasis in an RPL4 binding-dependent pattern. *Oncogene* 41: 3925-3938, 2022.
- Tian W, Du Y, Ma Y, Zhang B, Gu L, Zhou J and Deng D: miR663a-TTC22V1 axis inhibits colon cancer metastasis. *Oncol Rep* 41: 1718-1728, 2019.
- Jin MZ and Jin WL: The updated landscape of tumor microenvironment and drug repurposing. *Signal Transduct Target Ther* 5: 166, 2020.
- de Visser KE and Joyce JA: The evolving tumor microenvironment: From cancer initiation to metastatic outgrowth. *Cancer Cell* 41: 374-403, 2023.
- Pitt JM, Marabelle A, Eggermont A, Soria JC, Kroemer G and Zitvogel L: Targeting the tumor microenvironment: removing obstruction to anticancer immune responses and immunotherapy. *Ann Oncol* 27: 1482-1492, 2016.
- R Core Team: R: A language and environment for statistical computing. R Foundation for Statistical Computing, Vienna, Austria 2022.
- Fox J and Weisberg S: *An R Companion to Applied Regression*, Third edition. Sage, Thousand Oaks CA, 2019.
- Blanche P, Dartigues JF and Jacqmin-Gadda H: Estimating and comparing time-dependent areas under receiver operating characteristic curves for censored event times with competing risks. *Stat Med* 32: 5381-5397, 2013.
- Robin X, Turck N, Hainard A, Tiberti N, Lisacek F, Sanchez JC and Müller M: pROC: An open-source package for R and S+ to analyze and compare ROC curves. *BMC Bioinformatics* 12: 77, 2011.
- Bonneville R, Krook MA, Kautto EA, Miya J, Wing MR, Chen HZ, Reeser JW, Yu L and Roychowdhury S: Landscape of microsatellite instability across 39 cancer types. *JCO Precis Oncol* 2017: 17, 2017.
- Beroukhi R, Mermel CH, Porter D, Wei G, Raychaudhuri S, Donovan J, Barretina J, Boehm JS, Dobson J, Urashima M, *et al*: The landscape of somatic copy-number alteration across human cancers. *Nature* 463: 899-905, 2010.
- Mayakonda A, Lin DC, Assenov Y, Plass C and Koeffler HP: Maftools: Efficient and comprehensive analysis of somatic variants in cancer. *Genome Res* 28: 1747-1756, 2018.
- Love MI, Huber W and Anders S: Moderated estimation of fold change and dispersion for RNA-seq data with DESeq2. *Genome Biol* 15: 550, 2014.
- Gu Z, Gu L, Eils R, Schlesner M and Brors B: circlize Implements and enhances circular visualization in R. *Bioinformatics* 30: 2811-2812, 2014.
- Wu T, Hu E, Xu S, Chen M, Guo P, Dai Z, Feng T, Zhou L, Tang W, Zhan L, *et al*: clusterProfiler 4.0: A universal enrichment tool for interpreting omics data. *Innovation (Camb)* 2: 100141, 2021.
- Walter W, Sánchez-Cabo F and Ricote M: GOplot: An R package for visually combining expression data with functional analysis. *Bioinformatics* 31: 2912-2915.
- Thorsson V, Gibbs DL, Brown SD, Wolf D, Bortone DS, Ou Yang TH, Porta-Pardo E, Gao GF, Plaisier CL, Eddy JA, *et al*: The immune landscape of cancer. *Immunity* 48: 812-830.e14, 2018.
- Hänzelmann S, Castelo R and Guinney J: GSVA: Gene set variation analysis for microarray and RNA-seq data. *BMC Bioinformatics* 14: 7, 2013.
- Bindea G, Mlecnik B, Tosolini M, Kirilovsky A, Waldner M, Obenauf AC, Angell H, Fredriksen T, Lafontaine L, Berger A, *et al*: Spatiotemporal dynamics of intratumoral immune cells reveal the immune landscape in human cancer. *Immunity* 39: 782-795, 2013.
- Livak KJ and Schmittgen TD: Analysis of relative gene expression data using real-time quantitative PCR and the 2(-Delta Delta C(T)) method. *Methods* 25: 402-408, 2001.
- Loveday BPT, Lipton L and Thomson BN: Pancreatic cancer: An update on diagnosis and management. *Aust J Gen Pract* 48: 826-831, 2019.
- Cai J, Chen H, Lu M, Zhang Y, Lu B, You L, Zhang T, Dai M and Zhao Y: Advances in the epidemiology of pancreatic cancer: Trends, risk factors, screening, and prognosis. *Cancer Lett* 520: 1-11, 2021.
- Wood LD, Canto MI, Jaffee EM and Simeone DM: Pancreatic cancer: Pathogenesis, screening, diagnosis, and treatment. *Gastroenterology* 163: 386-402.e1, 2022.
- Chapa-González C, López K, Lomelí KM, Roacho-Pérez JA and Stevens JC: A review on the efficacy and safety of Nab-paclitaxel with gemcitabine in combination with other therapeutic agents as new treatment strategies in pancreatic cancer. *Life (Basel)* 12: 327, 2022.
- Xia T, Wu X, Cao M, Zhang P, Shi G, Zhang J, Lu Z, Wu P, Cai B, Miao Y and Jiang K: The RNA m6A methyltransferase METTL3 promotes pancreatic cancer cell proliferation and invasion. *Pathol Res Pract* 215: 152666, 2019.
- Lei Y, Yu T, Li C, Li J, Liang Y, Wang X, Chen Y and Wang X: Expression of CAMK1 and its association with clinicopathologic characteristics in pancreatic cancer. *J Cell Mol Med* 25: 1198-1206, 2020.
- Graham JB, Canniff NP and Hebert DN: TPR-containing proteins control protein organization and homeostasis for the endoplasmic reticulum. *Crit Rev Biochem Mol Biol* 54: 103-118, 2019.
- Chen M, Long Q, Borrie MS, Sun H, Zhang C, Yang H, Shi D, Gartenberg MR and Deng W: Nucleoporin TPR promotes tRNA nuclear export and protein synthesis in lung cancer cells. *PLoS Genet* 17: e1009899, 2021.
- Nie R, Liu Q and Wang X: TRPV1 Is a potential tumor suppressor for its negative association with tumor proliferation and positive association with antitumor immune responses in pan-Cancer. *J Oncol* 2022: 6964550, 2022.
- Xu X, Li N, Wang Y, Yu J and Mi J: Calcium channel TRPV6 promotes breast cancer metastasis by NFATC2IP. *Cancer Lett* 519: 150-160, 2021.
- Schizas D, Charalampakis N, Kole C, Economopoulou P, Koustas E, Gkotsis E, Ziogas D, Psyrri A and Karamouzis MV: Immunotherapy for pancreatic cancer: A 2020 update. *Cancer Treat Rev* 86: 102016, 2020.
- Bear AS, Vonderheide RH and O'Hara MH: Challenges and opportunities for pancreatic cancer immunotherapy. *Cancer Cell* 38: 788-802, 2020.
- Balan S, Saxena M and Bhardwaj N: Dendritic cell subsets and locations. *Int Rev Cell Mol Biol* 348: 1-68, 2019.
- Lee YS and Radford KJ: The role of dendritic cells in cancer. *Int Rev Cell Mol Biol* 348: 123-178, 2019.
- Gardner A, de Mingo Pulido Á and Ruffell B: Dendritic cells and their role in immunotherapy. *Fron Immunol* 11: 924, 2020.
- Wang S, Wu Q, Chen T, Su R, Pan C, Qian J, Huang H, Yin S, Xie H, Zhou L and Zheng S: Blocking CD47 promotes antitumor immunity through CD103 dendritic cell-NK cell axis in murine hepatocellular carcinoma model. *J Hepatol* 77: 467-478, 2022.
- Hegde S, Krisnawan VE, Herzog BH, Zuo C, Breden MA, Knolhoff BL, Hogg GD, Tang JP, Baer JM, Mpoy C, *et al*: Dendritic cell paucity leads to dysfunctional immune surveillance in pancreatic cancer. *Cancer Cell* 37: 289-307.e9, 2020.

42. Dongre A and Weinberg RA: New insights into the mechanisms of epithelial-mesenchymal transition and implications for cancer. *Nat Rev Mol Cell Biol* 20: 69-84, 2019.
43. Lüönd F, Sugiyama N, Bill R, Bornes L, Hager C, Tang F, Santacroce N, Beisel C, Ivanek R, Bürglin T, *et al*: Distinct contributions of partial and full EMT to breast cancer malignancy. *Dev Cell* 56: 3203-3221.e11, 2021.
44. Li S, Cong X, Gao H, Lan X, Li Z, Wang W, Song S, Wang Y, Li C, Zhang H, *et al*: Tumor-associated neutrophils induce EMT by IL-17a to promote migration and invasion in gastric cancer cells. *J Exp Clin Cancer Res* 38: 6, 2019.



Copyright © 2023 Ding et al. This work is licensed under a Creative Commons Attribution-NonCommercial-NoDerivatives 4.0 International (CC BY-NC-ND 4.0) License.